ISSN 2616-5775 Vol. 5, Issue 6: 1-6, DOI: 10.25236/AJCIS.2022.050601

Design and implementation of a three-port DC-DC converter

Dongyuan He[1,2], Jiachen Fan[1,2], Jiaxin He[1,2], Shihao Xian[1,2], Yong Hou[1,2]

[1]*College of Electronic Engineering, Guangxi Normal University, Guilin, China*
[2]*Original Power Technology Co., Guilin, China*

Abstract: *In order to resolve the problems of low efficiency and poor stability of traditional renewable energy systems, a three-port DC-DC converter for photovoltaic (PV) power systems and its control method are proposed in this paper. Firstly, the operating principles of the three-port DC-DC converter are analyzed in detail, and then, its topology are described. The proposed converter features simple topology, thus leading to high efficiency. Furthermore, the control method for the converter has been proposed for realizing constant voltage closed-loop control and maximum power point tracking (MPPT). Its operation can be transited mode automatically according to the photovoltaic power. Finally, the experimental data are given to verify the high efficiency and the feasibility of the converter.*

Keywords: *three-port DC-DC converter; PID; MPPT*

1. Introduction

With the increasing emphasis on environmental protection and the rapid development of modern technology, the application of renewable energy sources such as solar energy is increasing. However, the intermittent nature of the solar energy has hindered the wide promotion of these renewable energy sources. Therefore, an energy storage device is usually introduced in renewable energy power systems to convert the power of the PV, and such an approach can deal the challenge of intermittent nature of the renewable energy. Conventional renewable energy power systems typically require multiple DC-DC converters, resulting in increased size, relatively high cost and low efficiency. However, the three-port DC-DC converter is an excellent candidate for the renewable power system because of its small size and high efficiency compared to the traditional renewable energy power supply system [1-3]. The rest of this paper is structured as follows: section 2 analyzes the operating principle of the converter and presents the framework of the converter-based PV power system, section 3 introduces the topology of the converter, section 4 gives the control method, section 5 presents the experimental verifications, and section 6 concludes this paper.

2. Operating principle and system framework

2.1. The operating principle of the converter

According to the relationship between PV power and load demand power, the converter will operate in two operation modes. Therefore, the main function of the converter is to implement energy conversion between the three ports. These two operation modes are described as follows:

When the PV input power is higher than the load demand power, the converter will operate in single-input dual-output mode, which means that only the PV battery is the input source and the battery device can be regarded as an additional output in addition to the load. The input source will supply the load alone and use the remaining power to charge the battery device. The mode of operation is defined as mode 1.

When the PV input power is lower than the load demand power, the converter will operate in dual-input single-output mode, which means that the battery device will discharged to assist the input power to match the load demand power. The operating mode is defined as mode 2[4].

ISSN 2616-5775 Vol. 5, Issue 6: 1-6, DOI: 10.25236/AJCIS.2022.050601

2.2. Overall system framework

The system is composed of an simulated PV battery, an energy storage battery, a three-port DC-DC converter, and a variable load. Three ports of the converter are connected to one simulated PV battery, one energy storage battery and one load. The overall system framework is shown in Figure 1. In order to simulate the real lighting environment, the simulated PV battery is composed of one DC regulated power supply, one diode D1 and one resistor. The three-port DC-DC converter is composed of several circuits such as DC-DC synchronous rectifier circuit, STM32 control unit, auxiliary power supply circuit, switching tube driver circuit, and current and voltage sampling circuit.

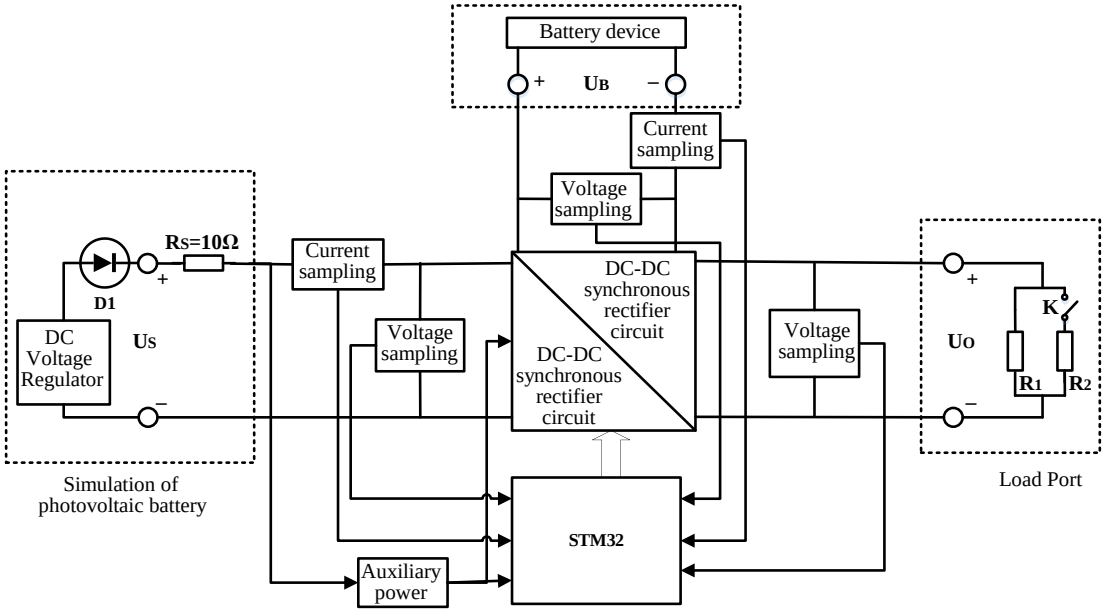

Figure 1: overall system framework

3. The topology of the converter

3.1. Auxiliary power supply circuit

In order to power the microcontroller, sampling chip and driver chip, an auxiliary power supply circuit is required to ensure stable operation of the circuit. The LM2576 series includes a fixed frequency oscillator (52kHz), a reference regulator (1.23V) and a complete protection circuit. The device requires only a minimal number of peripheral devices to form an efficient voltage regulator circuit. Therefore, the LM2576 integrated chip is used in this circuit.

3.2. DC-DC synchronous rectifier circuit

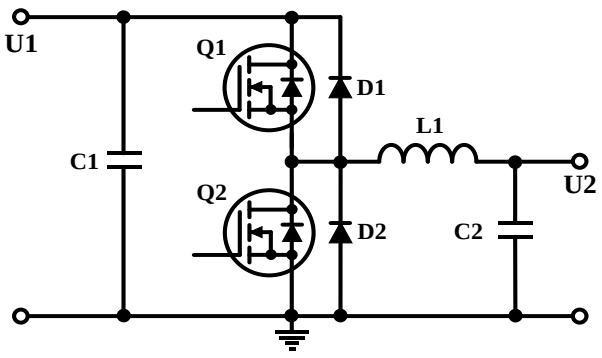

Figure 2: DC-DC synchronous rectifier circuit

ISSN 2616-5775 Vol. 5, Issue 6: 1-6, DOI: 10.25236/AJCIS.2022.050601

The DC-DC synchronous rectifier circuit is shown in Figure 2. The circuit uses a synchronous rectification scheme, so the efficiency of the converter can be greatly improved. The two MOSFETs Q1 and Q2 are controlled by a pair of complementary PWMs, thus the duty cycle of the PWMs can be adjusted to control the circuit. When the U1 port is the input and the U2 port is the output, this circuit is a BUCK circuit. When the U2 port is the input and the U1 port is the output, this circuit is a BOOST circuit. Because the model CSD19535KCS MOSFET has drain-source voltage is 100V, drain-source resistance is 0.0031Ω, and conduction loss is very small, so it was selected in the circuit.

3.3. MOSFET driver circuit

Since the MCU output does not have the ability to directly drive the MOSFETs, an additional driver circuit must be added. Here the IR2101 chip is selected as the core of the MOSFET driver circuit, the circuit is shown in Figure 4. The reason for choosing this device is that it has a highly integrated level conversion technology, which not only reduces the control parameters required by the logic circuit for the power device, but also greatly improves the stability of the driver circuit when working.

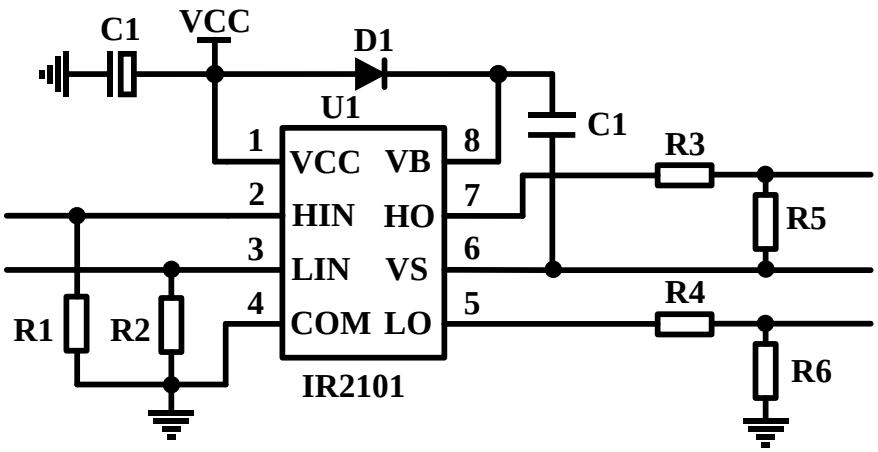

Figure 3: MOSFET driver circuit

3.4. DC current and DC voltage sampling circuit

For the STM32 MCU, its internal ADC can capture DC voltage signals in the range of 0V to 3.3V. If the voltage of the three ports of the converter is captured directly, it may be damaged. In addition, the ADC cannot capture DC current signals directly. A suitable sampling circuit is required to capture both the DC voltage signal and the DC current signal. For DC voltage sampling circuits, a resistor divider scheme can be used directly. For the DC current sampling circuit, use the MAX4080TASA chip to form a high-precision unidirectional current detection amplifier circuit to capture the current signal. The DC current sampling circuit is shown in Figure 3.

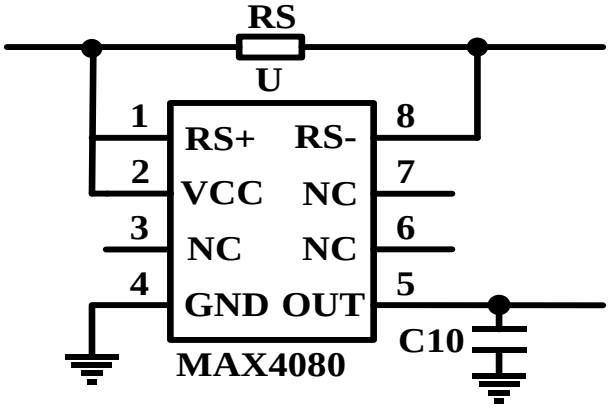

Figure 4: DC current and DC voltage sampling circuit

ISSN 2616-5775 Vol. 5, Issue 6: 1-6, DOI: 10.25236/AJCIS.2022.050601

4. Control method

4.1. Overall control process

First, the STM32 microcontroller captures the voltage and current signals from the three ports of the converter provided by the sampling circuit. Next, the microcontroller will process the data using a filtering algorithm to attenuate the effects of interfering noise. Then, the microcontroller will fit the filtered signals to obtain the approximate voltage and current values. Based on the current and voltage values, the PID and MPPT algorithms are used to obtain the appropriate pulse width size for the two pairs of PWM complementary waves, respectively. Finally, it is only necessary to output the two pairs of PWM complementary waves to the MOSFET drive circuit to get a stable DC voltage at the load as well as to achieve MPPT. The overall control flow is shown in Figure 5.

4.2. PID

In today's industrial control field, PID controller has become one of the most widely used controllers. Due to its simple principle, easy implementation, and simple parameters, it makes PID controllers suitable for most applications [5,6]. The incremental PID algorithm is used in this system, which requires only the last three sampled values to obtain the control increment and can avoid the phenomenon of integral saturation [7]. The expression is shown in equation 1.

$$\Delta u(k) = [(e(k) - e(k-1)) + \frac{1}{T_i} e(k) + T_d (e(k) + 2e(k-1) + e(k-2))] \tag{1}$$

4.3. MPPT

In fact, PV cells have significant nonlinear characteristics. Therefore, in order to maximize the output power of the PV system, it is necessary to control the PV cell with MPPT [8]. In this paper, the MPPT is implemented in the three-port DC-DC converter using the perturbation observation method. This is the most common single-peak maximum power point tracking method, and its basic principle is as follows. First, the output voltage and current values at that moment are sampled to calculate the current output power. Then, adjust the duty cycle of the synchronous rectifier circuit, apply a small disturbance to the output voltage, and sample the voltage and current of the load at this time and calculate the power value. Finally, the current moment and the previous moment sampling calculated power value for comparison, if the output power increases, that the perturbation direction is correct, is close to the maximum power point, the next moment to keep the perturbation direction unchanged to apply perturbation; if the output power decreases, that is far from the maximum power point, it is necessary to adjust the perturbation direction, the next moment to the current perturbation direction of the opposite direction to apply perturbation. By this method, the maximum power point can be approached continuously until the PV cell finds the maximum power point and operates stably at the maximum power point [9].

5. Experimental verifications

To verify the feasibility and high efficiency of the proposed three-port DC-DC converter, a high-power prototype has been built and extensive experiments have been conducted. The idea of the experiment is as follows. Varying the simulated sunlight intensity (U_S) and the load, we test whether the converter can automatically switch the operating mode, whether the output voltage (U_o) can be stabilized at 30V, and whether the converter can operate near the maximum power point. Finally, the performance of the converter is calculated by analyzing each data.

5.1. Efficiency

The parameters of the ports of the proposed converter at $U_S = 50\text{V}$ and $I_O = 1.2\text{A}$ are shown in Table 1.

Table 1: Parameters for Mode I efficiency test.

U_I (V)	I_I (A)	U_B (V)	U_B (A)	U_O (V)	I_O (A)
24.37	2.46	16.48	1.36	29.92	1.17

ISSN 2616-5775 Vol. 5, Issue 6: 1-6, DOI: 10.25236/AJCIS.2022.050601

At this time, the converter is in Mode I, and the PV battery supplies power to both the load and the battery, as is shown in

$$\eta_{\mathrm{I}} = \frac{P_O + P_B}{P_I} \times 100\% \tag{2}$$

Therefore, the η_{I} is calculated to be 95.78%

The parameters of the ports of the proposed converter at $U_S = 50\mathrm{V}$ and $I_O = 1.2\mathrm{A}$ are shown in Table 2.

Table 2: Parameters for Mode II efficiency test.

U_I (V)	I_I (A)	U_B (V)	U_B (A)	U_O (V)	I_O (A)
24.11	1.00	14.86	-0.81	29.90	1.16

At this time, the converter is in Mode II, and the PV battery and battery power the load at the same time, as is shown in

$$\eta_{\mathrm{II}} = \frac{P_O}{P_I + P_B} \times 100\% \tag{3}$$

Therefore, the η_{II} is calculated to be 95.95%

5.2. Voltage adjustment rate and MPPT

The tested parameters of the ports of the proposed converter are shown under the conditions of $I_O = 1.2\mathrm{A}$ and reduction of U_S from 55V to 25V in Table 3.

Table 3: Measurement of voltage regulation and verification of MPPT parameters.

U_S (V)	U_I (V)	U_O (V)
54.32	27.31	30.03
24.47	12.32	30.06

The deviation from the maximum power point is given by

$$\delta_{U_I} = \left| U_I - \frac{U_S}{2} \right| \tag{4}$$

The deviation from the maximum power point is calculated to be 0.15 V and 0.085 V for the two conditions, respectively.

The voltage adjustment rate is given by

$$S_U = \left| \frac{U_{O55} - U_{O25}}{U_{O25}} \right| \times 100\% \tag{5}$$

The voltage adjustment rate calculated voltage regulation is 0.1%.

5.3. Load adjustment rate

The tested parameters of the ports of the proposed converter are shown under the conditions of $U_S = 35\mathrm{V}$ and reduction of I_O from 1.2A to 0.6A in Table 4.

Table 4: Parameters for measuring the load regulation rate.

I_O (A)	U_O (V)
1.2	29.93
0.6	29.95

The load adjustment rate is given by

$$S_I = \left| \frac{U_{O0.6} - U_{O1.2}}{U_{O1.2}} \right| \times 100\% \tag{6}$$

ISSN 2616-5775 Vol. 5, Issue 6: 1-6, DOI: 10.25236/AJCIS.2022.050601

Therefore, the load adjustment rate is calculated to be 0.07%.

6. Conclusions

In this paper, a three-port DC-DC has been proposed for simultaneous connection of PV port, battery and load port. The operating principle of the converter has been analyzed in detail, and the its control method have been given. Depending on the solar power and load power demand, the converter will change mode automatically. Finally, a low-power prototype has been built, and the effectiveness and high efficiency of the proposed topology with the control method has been verified by the experimental results. The proposed converter can be applied in the PV power system.

References

[1] Zhu H, Zhang D, Zhang B, et al. A nonisolated three-port DC–DC converter and three-domain control method for PV-battery power systems [J]. IEEE Transactions on Industrial Electronics, 2015, 62(8): 4937-4947.

[2] Wang Z, Li H. An integrated three-port bidirectional DC–DC converter for PV application on a DC distribution system [J]. IEEE Trans Power Electron, 2013, 28(10): 4612-4624.

[3] SONG Xin, XIAO Jianguo, NIU Jieru, et al. A phase-shift controlled three-port DC-DC converter for new energy hybrid generation [J]. Transactions of China Electrotechnical Society, 2015, 30(17): 36-44.

[4] Zhang N, Sutanto D, Muttaqi K M. A review of topologies of three-port DC–DC converters for the integration of renewable energy and energy storage system [J]. Renew Sustain Energy Rev, 2016, 56: 388-401.

[5] Wang Yichen. Comparison and research on the adjustment of incremental PID and positional PID algorithms [J]. Industrial Control Computer, 2018, 31(5): 123-124.

[6] Wu Hongxin, Shen Shaoping. Application and theoretical basis of PID control [J]. Control Engineering of China, 2003 (01): 37-42.

[7] Jin Fu'an. Differential and integral saturation problems in digital PID algorithms [J]. Microcomputer Development, 2001(06): 6-8.

[8] Xu P.W., Liu F., Liu B.Y., Duan S.X.. Analytical comparison and improvement of several MPPT methods for photovoltaic systems [J]. Power Electronics, 2007(05): 3-5.

[9] Li Fujun. Research on maximum power point tracking control method for photovoltaic power generation system [D]. Hunan University of Technology, 2020.